

ON DECOMPOSITION OF AMORPHOUS PHASE IN METALLIC GLASSES

G. Abrosimova and A. Aronin

Institute of Solid State Physics RAS, Chernogolovka, Russia

Received: March 10, 2016

Abstract. Structure evolution in metallic glasses under heating and deformation is studied and discussed. Special attention is devoted to the pre-crystallization processes occurring at heating and deformation. A separation of uniform amorphous phase and formation of regions with different type of short range order and/or different composition in light amorphous Al-Ni-RE (RE = La, Gd or Y) alloys is described. Possible reasons of amorphous phase decomposition are considered.

1. INTRODUCTION

Amorphous metallic alloys or metallic glasses have already been the subject of intensive research over a number of years [1-10]. The interest to these materials is determined by their structure, a complex of unique physicochemical properties in certain cases and the feasibility of using them as a basis for producing composite amorphous-nanocrystalline materials [11-16]. Nanostructured materials are produced by different methods, the parent structures being amorphous and crystalline materials that attract increasing researchers' interest and stimulate studies aimed at creating novel materials with enhanced physicochemical properties [17-19]. A large group of nanomaterials are already used commercially [20, 21].

One of the main methods of creating nanocrystalline materials is controlled crystallization of amorphous alloys obtained by rapid melt quenching onto a moving substrate. The samples are produced as continuous ribbons with a homogeneous amorphous structure. Yet, when exposed to thermal or deformation effects under non-

crystallization conditions, the amorphous phase structure may change significantly and contain regions that are different in composition and short-range order type, i.e. co-existence of several amorphous phases is observed [22-26]. So far the inhomogeneous amorphous phase has been observed in some systems, but only last years with appearance of such novel objects as nanoglasses encouraged systematic research. $\text{Pd}_{74}\text{Au}_8\text{Si}_{18}$ [22], $\text{Pd}_{40.5}\text{Ni}_{40.5}\text{P}_{19}$ [23], $\text{Be}_{40}\text{Ti}_{24}\text{Zr}_{36}$ [24] were among the first alloys in which an inhomogeneous amorphous phase was discovered. The X-ray and electron diffraction patterns of Al-Si-X and Al-Ge-X metallic glasses (X = Ti, Zr, V, W, Mn, Fe, Co, Ni, Cu, Cr, Nb, Mo) [27] exhibited a double halo, and in $\text{Al}_{70}\text{Si}_{20}\text{Ni}_{10}$ the scattering vectors corresponding to the two diffusion maxima were essentially different (0.269 ± 0.003 and $0.322 \pm 0.003 \text{ nm}^{-1}$). The analysis made enabled to conclude that the smaller angle peak was determined by the primary Al-Al neighbors and the larger angle peak by the Si-(Al,X) or Ga-(Al, X) neighbors. The data of high resolution electron microscopy show that the structure displays an inhomogeneous distribution of atoms on the near-

Corresponding author: G. Abrosimova, e-mail: gea@issp.ac.ru

10 Å scale, which was related to formation of aluminum insoluble silicon and germanium clusters. Inhomogeneities were also discovered in (Au-Pb-Pt) – (Pb-Sb) [28], Pd-Si-Sb and other alloys [29].

Inhomogeneities were observed not only in as-prepared amorphous structure. In some cases structural inhomogeneities occurred as a result of various external actions such as heating, irradiation, etc. For instance, in the Pd-Au-Si alloy as-prepared amorphous phase was initially homogeneous, yet, 400 °C annealing caused phase separation into regions of different elemental composition [30]: the $(\text{Mo}_{0.6}\text{Ru}_{0.4})_{100-x}\text{B}_x$ alloy [5] exhibited formation of chemical segregations prior to the onset of crystallization. The studies of $\text{Fe}_{67}\text{Co}_{18}\text{B}_{14}\text{Si}_1$ alloy structure revealed that the as-prepared amorphous phase is homogeneous but its heating up to 400-600 °C brings about formation of boron-enriched regions and those of Fe-Co composition [31], i.e. regions with different types of short-range order. Short-range order is clearly dependent on the chemical composition. The changes of the short-range order with varying composition were investigated by some authors. For instance, work [14] addressed research into the changes of amorphous $(\text{Zr}_{0.667}\text{Ni}_{0.333})_{1-x}\text{B}_x$ alloy structure with varying boron content from 0 to 25 at.%. It was shown that the short-range order type changes at $x \approx 0.05$.

Irradiation of amorphous alloys with fast neutrons, for instance, can also lead to formation of inhomogeneous amorphous structure composed of regions with different short-range order. Irradiation of amorphous $\text{Pd}_{80}\text{Si}_{20}$ alloy with a fast neutron dose of $5 \cdot 10^{20}$ neutron/nm² resulted in formation of structural inhomogeneities as high-electron-density clusters surrounded by boundary regions with lower electron density. The diameter of the clusters including the shell was 10-20 Å [32]. Irradiation may result not only in formation but also reduction of inhomogeneities.

A significant amount of data of the studies of amorphous phase inhomogeneities was obtained using the small angle X-ray scattering technique. Annealing of amorphous $\text{Fe}_{90}\text{Zr}_{10}$ alloy caused an increase in small angle X-ray scattering. During annealing at 653 °C for 10 min the size of the inhomogeneity regions increased from 6 to 12 Å [33]. A significant increase in small angle X-ray scattering intensity on heating the same alloy until the onset of crystallization was also observed by other researchers [34]. Increased small angle X-ray scattering intensity in the amorphous state was observed in Fe-P-C, Fe-B, Pd-Au-Si and other alloys [35]. It is interesting to note that occurrence of

inhomogeneities may be related to the composition of the amorphous phase. For instance, in amorphous Cu-Ti and Ni-Y alloys small angle X-ray scattering in the amorphous phase was discovered in compositions that did not correspond to the crystalline phases on the phase diagrams and was absent when the composition of the amorphous phase corresponded to that of the precipitating crystalline phases [36]. Small angle X-ray scattering intensity usually increases with increasing temperature or annealing duration. This process is obviously conditioned by structural rearrangements within the amorphous phase, formation of regions with a chemical composition and/or short-range order different from those of the matrix, i.e. actual formation of several amorphous phases. Inhomogeneity regions form not only on heating but also under deformation [17,37].

The scale of decomposition (or the size of regions with different amorphous phases) may vary over a wide range from ~ 2-5 nm [38] to ~ 50 nm [25] depending on alloy composition and conditions of thermal treatment. The changes occurring in the amorphous phase structure before the onset of crystallization may significantly affect the morphology and parameters of the crystalline structure forming on subsequent heating [39-41]. Another example is the observed 10-fold increase of the crystal size in the Fe-B alloy after preliminary (precrystallization) annealing [39] or the possibility of preparing amorphous samples with crystalline surfaces or crystalline samples with amorphous surface in Fe-B-P alloys [40]. Since the changes proceeding in the amorphous matrix before the onset of crystallization may essentially influence the parameters of the crystalline structure, it is important to investigate such changes in alloys of different chemical composition. We have previously studied the changing degree of amorphous phase decomposition in $\text{Al}_{87}\text{Ni}_8\text{La}_5$ alloy during isothermal annealing as well as evolution of amorphous phase structure in different Al-Ni –RE (RE = La, Gd or Y) alloys in the course of thermal treatment and deformation [42]. This paper studies the evolution of the amorphous structure in different Al-Ni -RE (RE = La, Gd or Y) alloys during heat treatment and deformation.

2. EXPERIMENTAL

Alloy ingots of $\text{Al}_{87}\text{Ni}_8\text{La}_5$, $\text{Al}_{87}\text{Ni}_8\text{Gd}_5$ and $\text{Al}_{87}\text{Ni}_8\text{Y}_5$ composition were prepared by arc melting as a preliminarily master alloy. Amorphous ribbons about 30 µm thick and ~20 mm wide were made by the

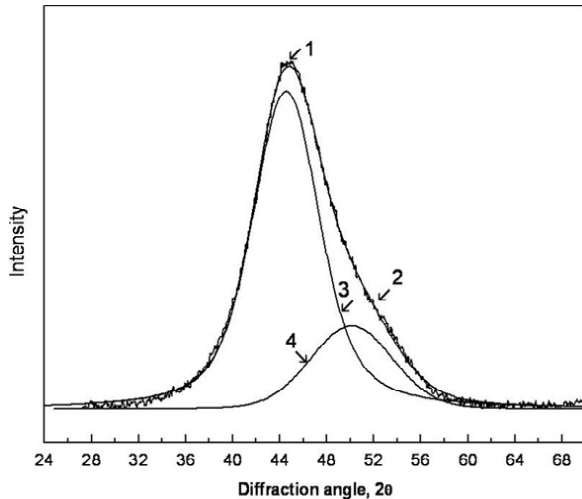


Fig. 1. X-ray diffraction pattern of amorphous $\text{Al}_{87}\text{Ni}_8\text{La}_5$ alloy annealed at 150 °C for 15 h; 1 – experimental spectrum, 2 – summary curve, 3 and 4 – diffuse halos from the first and second amorphous phases.

single roller melt spinning technique in a helium atmosphere. The samples were annealed in a resistance furnace at different temperatures. Deformation was performed in a VEB Schwermaschinenbau four-roll mill by the multiple rolling technique, the run number being 50-150. The deformation value was calculated by the formula $\varepsilon = \Delta h/h_0$, where h_0 and Δh are the original thickness and its deformation-induced change, respectively.

The differential scanning Perkin Elmer DSC7 calorimeter was used for the study of the thermal stability of the samples. The measurements were carried out at temperatures up to 500 °C with a heating rate of 20 K/min. The structure of the as-prepared, deformed and annealed samples was studied by X-ray diffraction using a SIEMENS D-500 diffractometer with Co K_α - radiation. Special computer programs were used for smoothing and background correction. The microstructure was studied by transmission electron microscopy using a JEM-100CX electron microscope.

3. RESULTS AND DISCUSSION

The characteristics of formation of several amorphous phases in alloys with different rare earth components were studied using a group of Al-Ni-RE alloys (lanthanum, gadolinium, yttrium). The atomic sizes of the rare earth metals are significantly different ($R_Y = 1.810 \text{ \AA}$, $R_{\text{Gd}} = 1.802 \text{ \AA}$, $R_{\text{La}} = 1.877 \text{ \AA}$), hence, it would be natural to expect that the component redistribution processes may be

different. As it was shown in [42], annealing of amorphous $\text{Al}_{87}\text{Ni}_8\text{La}_5$ alloy at 150 °C changes the amorphous phase structure: the X-ray diffraction pattern exhibits a shoulder on the large angle side, the degree of the maximum distortion increases with annealing time. Upon thermal treatment the diffuse maximum is a superposition of two maxima (Fig. 1).

The main structural changes occur during the first hours of annealing, following which the structures remain practically unchanged. The shortest interatomic distances in the amorphous phase calculated with the use of the Ehrenfest equation [43],

$$2R_1 \sin\theta = 1.23\lambda,$$

(R_1 is the radius of the first coordination sphere, 2θ the angle of reflection, λ the radiation wavelength) in the two formed amorphous phases are 2.98 Å and 2.54 Å. It is clear that the phase with the largest interatomic distance is enriched with lanthanum (the largest atom in the system).

Similar changes were observed after isothermal annealing of amorphous $\text{Al}_{87}\text{Ni}_8\text{Y}_5$ alloy at 100 °C. It was established that the decomposition of the amorphous phase in the $\text{Al}_{87}\text{Ni}_8\text{Y}_5$ alloy starts immediately with annealing and increases insignificantly with increasing annealing time: as the duration of annealing increases from 3 to 30 h, the difference in the positions of the main and extra diffuse maxima (shoulder) increases by 2.5%. This change is attended with an increasing fraction of the new ("second") amorphous phase. As in the case of the lanthanum alloy, low temperature annealing of the amorphous yttrium alloy leads to decomposition of the amorphous phase into rare earth component-enriched and -depleted regions. The newly formed amorphous regions are distinguished by different radii of the first coordination sphere (different shortest interatomic distances), which is revealed by the occurrence and growth of the shoulder on the main diffuse maxima in the X-ray diffraction patterns. The angular difference in the positions of the main and extra peaks in the $\text{Al}_{87}\text{Ni}_8\text{La}_5$ alloy is $\Delta 2\theta = 6.7$ and $\Delta 2\theta = 6.3$ in the $\text{Al}_{88}\text{Ni}_6\text{Y}_6$ alloy.

Fig. 2 presents the initial parts of the X-ray diffraction patterns of the alloys in question (the first maximum region after thermal treatment). The inset shows the decomposition of the diffuse maximum for the $\text{Al}_{87}\text{Ni}_8\text{Gd}_5$ alloy. It is seen that the thermal treatment of all the alloys results in distortion of the diffuse maximum in the X-ray diffraction patterns.

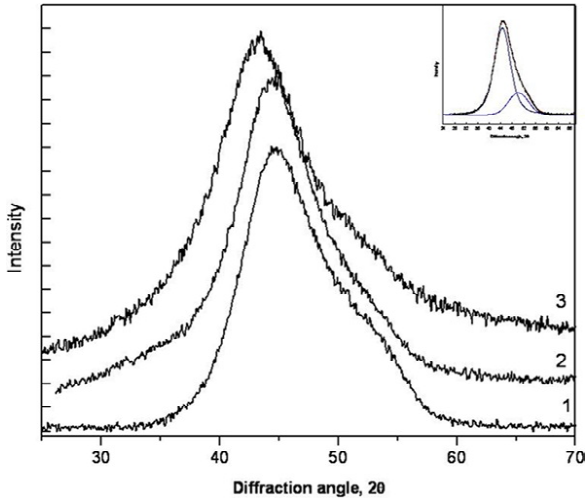


Fig. 2. X-ray diffraction patterns of annealed amorphous $\text{Al}_{87}\text{Ni}_8\text{Y}_5$ (1), $\text{Al}_{87}\text{Ni}_8\text{Gd}_5$ (2 and inset) and $\text{Al}_{87}\text{Ni}_8\text{La}_5$ alloys (3). The inset presents decomposition of the diffuse maximum for $\text{Al}_{87}\text{Ni}_8\text{Gd}_5$ alloy.

The changes of the amorphous phase induced by plastic deformation were also investigated. Deformation was carried out by multiple rolling, the maximum degree of deformation was about 40%. The decomposition of the amorphous structure in the course of plastic deformation for the $\text{Al}_{87}\text{Ni}_8\text{Y}_5$ and $\text{Al}_{87}\text{Ni}_8\text{Gd}_5$ alloys is shown in Fig. 3 (Figs. 3a and 3b, respectively). It is seen that, as in the case of thermal treatment, deformation results in decomposition of the amorphous matrix into regions of different chemical composition and/or short-range order. Under deformation the observed degree of decomposition (the difference in the positions of the main and extra diffuse halos in the X-ray diffraction patterns) was less than that upon thermal treatment and increased slightly with increasing deformation degree.

The known statement that the positions of the maxima on the scattering curves determine the radius of first coordination sphere R_1 ,

$$R_1 = 7.73/(S_1)_{\max} = 14.06/(S_2)_{\max} = 20.46/(S_3)_{\max} \dots\dots,$$

(where $(S_1)_{\max} = 4\pi(\sin\theta/\lambda)$ is the wave vector corresponding to the first (second, third... maximum of the intensity curve), θ the scattering angle, λ the radiation wavelength) was used to determine the radii of the coordination spheres of the amorphous phases on termination of the decomposition process. The results obtained are presented in Table 1.

As mentioned above, the presence of two diffuse maxima suggests the presence of amorphous matrix

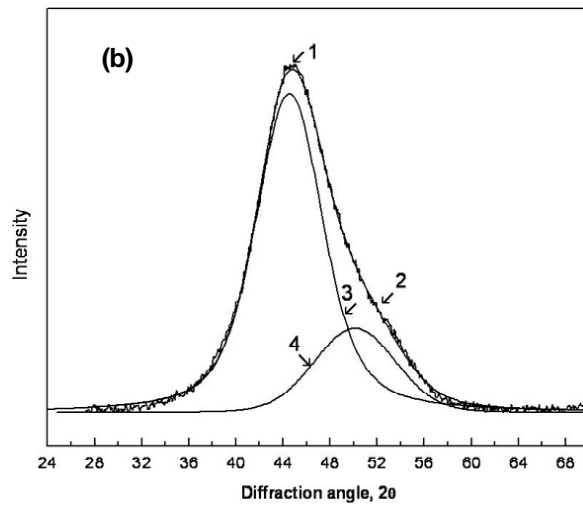
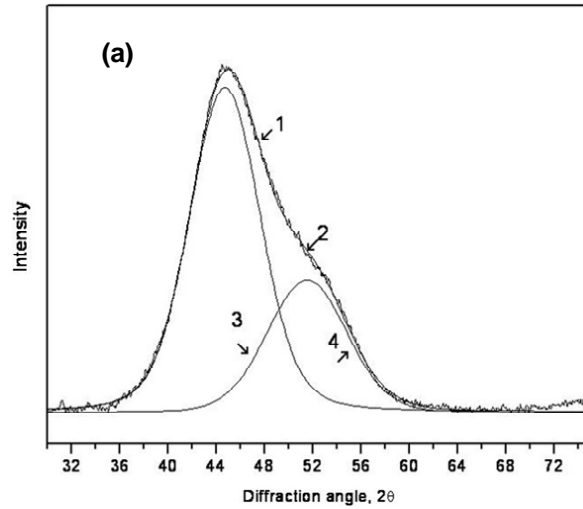


Fig. 3. X-ray diffraction patterns of deformed samples of amorphous $\text{Al}_{87}\text{Ni}_8\text{Y}_5$ (a) and $\text{Al}_{87}\text{Ni}_8\text{Gd}_5$ alloys (b): 1 – experimental spectrum, 2 – summary curve, 3 and 4 – diffuse halos from first and second amorphous phases.

regions with different radii of the first coordination sphere. The different angular positions of the diffuse maxima are indicative of formation of amorphous regions of different chemical composition, i.e. formation of two amorphous phases. In all the three alloy systems the maximum located at smaller angles corresponds to the amorphous phase with a large radius of the first coordination sphere (or the largest interatomic distance in the amorphous phase). Since in the system studied the largest atoms are those of the rare earth components (radii $R_{\text{Ni}} = 1.246 \text{ \AA}$, $R_{\text{Al}} = 1.431 \text{ \AA}$), this amorphous phase is enriched with rare earth metals.

The data obtained are in good agreement with the results of the TEM studies of the samples. Fig. 4 presents the electron diffraction pattern of the deformed $\text{Al}_{87}\text{Ni}_8\text{Gd}_5$ alloy sample. It is seen that the

Table 1. Radii of the first coordination sphere for as-prepared amorphous phases (R_0) and for amorphous phases (R_1 and R_2) after annealing.

Alloy	R_0 , Å.	Treatment	R_1 , Å.	R_2 , Å.	ΔR , Å
$\text{Al}_{87}\text{Ni}_8\text{La}_5$	2.97	Annealing	2.98	2.54	0.44
$\text{Al}_{87}\text{Ni}_8\text{Y}_5$	2.89	Annealing	2.90	2.56	0.34
$\text{Al}_{87}\text{Ni}_8\text{Y}_5$	2.89	Deformation	2.90	2.58	0.32
$\text{Al}_{87}\text{Ni}_8\text{Gd}_5$	2.88	Annealing	2.91	2.61	0.30
$\text{Al}_{87}\text{Ni}_8\text{Gd}_5$	2.88	Deformation	2.90	2.55	0.35

diffusion halo is “double”, which points to two values of the shortest interatomic distance, i.e. the presence of two amorphous phases.

Thus, the process of low temperature annealing and deformation involves redistribution of the components in the amorphous phase leading to formation of regions of different chemical composition:

- low temperature annealing prior to the onset of crystallization gives rise to regions of inhomogeneous chemical composition (amorphous regions distinguished by different radii of the first coordination sphere) of the Al-Ni-La, Al-Ni-Y system;
- structural changes are slower with increasing atomic size of the rare earth component (decreased diffusion coefficient);
- rolling deformation could also cause decomposition of the amorphous phase even at room temperature (Al-Ni-Y, Al-Ni-Gd systems).

When analyzing the dependence of the decomposition processes on alloy composition, a number of parameters should be taken into account: atomic size (and, hence, the rate of diffusion mass transfer), mixing enthalpy of the components, the position of the composition in question on the phase equilibrium diagrams, compositional complexity

**Fig. 4.** Electron diffraction pattern of the deformed $\text{Al}_{87}\text{Ni}_8\text{Gd}_5$ sample.

(number of components). As regards atomic sizes, it seemed natural to observe slowdown of the decomposition process in the case of the amorphous phase containing a rare earth component with the largest atomic size. However, the diffusion coefficient is a kinetic parameter and can determine only the rate of the process when the corresponding potentialities are given. One of the most important thermodynamic characteristics is mixing enthalpy of the components. In the systems investigated the component mixing enthalpies are negative and differ only slightly: -38 kJ/mole for Al-La and Al-Y pairs, -39 kJ/mole for Al-Gd, -22 kJ/mole for Al-Ni, -27 kJ/mole for Ni-La, -31 kJ/mole for Ni-Gd and Ni-Y pairs [44]. In several recent works it has been shown that if there is positive or slightly negative mixing enthalpy between two atoms in the multicomponent amorphous phase, it will exhibit a decomposition tendency. The above values of mixing enthalpy show that the alloys under study do not belong to that group. Therefore, decomposition is not determined merely by mixing enthalpy.

The specific features of structural changes are conditioned by the phase equilibrium diagram, on the one hand (although it is not always the case in amorphous metallic alloys), and compositional complexity (number of components), on the other hand. It is known that at the initial stage of crystallization of the amorphous phase of hypoeutectic composition usually follows the phase equilibrium diagram, while crystallization of the amorphous phase of hypereutectic composition, as a rule, does not correspond to the phase equilibrium diagram. The compositions of all the investigated alloys are hypereutectic and it could be expected that crystallization of the amorphous phase would start with formation of crystals of corresponding intermetallic compounds. Yet, in all the cases the initial stage always exhibits precipitation of aluminum crystals.

It should be noted that crystallization of metallic glasses often starts with formation of metastable phases, some of them forming only on crystallization

of the amorphous phase and not in any other conditions [45]. One of the criteria for amorphous phase stability is related to the similarity of the short-range order in the amorphous alloy and that in the forming crystalline phases. Since phase transformation usually follows the nucleation and growth mechanisms, the size of the critical nucleus is crucial. The smaller the size of the critical nucleus, the smaller the fluctuations of the short-range order and/or composition required for its formation. The minimal size of the critical nucleus of the crystalline phase is the size of its unit cell. If crystallization produces complex phases with a large number of atoms in the unit cell and large cell parameters, then formation of a critical nucleus requires large fluctuations, which will result in higher amorphous phase stability. Hence, higher amorphous phase stability is characteristic of metallic glasses whose short-range order corresponds to that of crystalline phases with a large lattice parameter and complex structure.

The systems investigated could be compared to those belonging to amorphous alloys with a high vitrification tendency. The classical example is Zr-Ni-Be-... type alloys that are used to produce bulk metallic glasses. The mixing enthalpies for Zr-Ni and Zr-Be are equal to -49 and -43 kJ/mole, respectively [44]. These values are distinctly smaller than the corresponding values for the investigated alloys. It means that in the systems in question the probability of decomposition may be significantly higher. Besides, comparison of mixing enthalpies for components of yttrium-containing alloys reveals that the value of the mixing enthalpy for Al-Y (-38 kJ/mole) is smaller than the corresponding values for Al-Ni (-22 kJ/mole) and Ni-Y (-31 kJ/mole). Therefore, the binary alloy is likely to exhibit a lower degree of decomposition of the amorphous phase than the ternary alloy, which is in agreement with the experimental data [46].

Before cooling the melt contains co-existing clusters with different types of short-range order and of different chemical composition. The structure of the amorphous phase inherits that of the melt before quenching. Heating or any other action induces ordering based on the existing regions with various types of short-range order. The melt of near-eutectic composition contains atomic groups or different types of clusters which are sites of easier formation of ordered regions and then same types of crystals. It is known, for instance, that formation of aluminum nanocrystals in aluminum - transition metal - rare earth metal alloy systems starts in metal-rare earth component-depleted sites [40,47]. The more

components there are in the alloy, the more diverse are the configurations in the melt. Formation of atomic clusters is also determined by the sign and value of mixing enthalpy. Therefore, when considering the values of mixing enthalpy of the alloy components, it should be noted that in the binary alloy the negative mixing enthalpy of the Al-Y components is the largest, which does not facilitate decomposition of the amorphous phase.

4. CONCLUSIONS

Thus, the data available in literature and our experimental results on decomposition of metallic glasses enable to make the following conclusions. Decomposition is observed in alloys whose components reveal positive as well as negative mixing enthalpy. The data obtained show that the decomposition criterion related to the value of mixing enthalpy does not exhaust all feasible causes of decomposition. It is based on the approach that the free alloy energy will decrease with decomposition. This will occur if there is a possibility, for example, at long-term relaxation. In the cases considered the system acquires extra energy either owing to heating or deformation. It is clear that the system therewith can deviate from equilibrium and be, in principle, subject to decomposition.

ACKNOWLEDGEMENTS

The work was partially supported by the Russian Foundation for Basic Research (grants 16-03-00505, 17-43-500809).

REFERENCES

- [1] A.L.Greer // *Acta Metall.* **30** (1982) 171.
- [2] Y. Khan and M. Sostarich // *Z. Metallk.* **72** (1981) 266.
- [3] G.E.Abrosimova, A.S.Aronin, S.P.Pankratov and A.V.Serebryakov // *Scr. Metall.* **14** (1980) 967.
- [4] A. Mak, K. Samwer and W.L. Johnson // *Phys. Lett.* **98A** (1983) 353.
- [5] M. Mehra, R. Schulz and W.L. Johnson // *J. Non-Crystall. Solids* **61-62** (1984) 859.
- [6] A.R. Yavari // *Acta Metall.* **36** (1988) 1863.
- [7] G.E. Abrosimova, A.S. Aronin, V.E. Asadchikov, S.P. Pankratov and A.V. Serebryakov // *Fizika metalov i metallovedenie* **62** (1986) 496.
- [8] A.R. Yavari, K. Osamura and H. Okuda // *Phys. Rev. B.* **37** (1988) 7759.

- [9] G.E. Abrosimova, A.S. Aronin and E.Yu. Ignat'eva // *JMMM* **203** (1999) 169.
- [10] V. Cremaschi, B. Arcondo and H. Sirki // *J Mater. Res.* **15** (2000) 1936.
- [11] Y.He, J.F.Poon and G.Y.Shiflet // *Science* **241** (1988) 1640
- [12] A.Inoue, T.Ochiai, Y.Horio and T.Masumoto // *Mater. Sci. Eng. A* **179/A180** (1994) 649
- [13] I.S. Tereshina, E.A. Tereshina, G.S. Burkhanov and S.V. Dobatkin // *Rev. Adv. Mater. Sci.* **25** (2010) 82.
- [14] Y.H.Kim, A.Inoue and T.Masumoto // *Mater. Trans. J I M* **32** (1991)331.
- [15] D.V.Louzguine and A.Inoue // *J.Non-Cryst. Solids* **311** (2002) 281.
- [16] A.S. Aronin, G.E. Abrosimova and Yu.V. Kir'yanov // *Physics of the Solid State* **43** (2001) 2003.
- [17] A. Aronin, G. Abrosimova, D. Matveev and O. Rybchenko // *Rev. Adv. Mater. Sci.* **25** (2010) 52.
- [18] Q. Zheng // *Rev. Adv. Mater. Sci.* **40** (2015) 1.
- [19] T.G. Langdon // *Rev. Adv. Mater. Sci.* **31** (2012) 1.
- [20] T.G. Langdon // *Rev. Adv. Mater. Sci.* **25** (2010) 11.
- [21] A. Khitab and M. Tausif // *Rev. Adv. Mater. Sci.* **38** (2014) 181.
- [22] C-P. Chou and D. Turnbull // *J. Non-Cryst. Solids* **17** (1975) 169
- [23] H.S. Chen // *Mater. Sci. Eng.* **23** (1976)151
- [24] L. Tanner and R. Ray // *Scr. Metall.* **14** (1980)657
- [25] G.E. Abrosimova, F.S. Aronin and E.Yu. Ignat'eva // *Physics of the Solid State* **48** (2006) 563.
- [26] G.E. Abrosimova and A.S. Aronin // *Physics of the Solid State* **40** (1998) 1603.
- [27] A. Inoue, M. Yamamoto, H. Kimura and T. Masumoto // *J. Mater. Sci.* **6** (1987) 194.
- [28] A. R. Yavari // *Acta Metall.* **36** (1988) 1863.
- [29] M. Marcus // *J. Non-Cryst. Solids* **30** (1979) 317.
- [30] H.S. Chen and D. Turnbull // *Acta Metal.* **17** (1969) 1021.
- [31] T. Nagarajan, U. Asari, S. Srinivasan, V. Sridharan and A. Narayanasamy // *Hyperfine Interactions* **34** (1987) 491
- [32] K. Doi, H. Kayano and T. Masumoto // *J. Appl. Cryst.* **11** (1978) 605.
- [33] H. Terauchi // *J. Phys. Soc. Jap.* **52** (1983) 3454.
- [34] K. Osamura // *J. Mater. Sci.* **19** (1984) 1917.
- [35] H. Hermann, N. Mattern, U. Kuhn, A. Heinemann and N.P. Lazarev // *J. Non-Crystalline Solids* **317** (2003) 91.
- [36] H.W. Sheng // *Nat Mater.* **6(3)** (2007) 192.
- [37] A.S. Aronin and G.A. Abrosimova // *Mater. Let.* **83** (2012) 183.
- [38] A.S. Aronin, G.E. Abrosimova, A.F. Gurov, Yu.V. Kir'yanov and V.V. Molokanov // *Mater. Sci. Eng. R* **304-306** (2001) 375.
- [39] G.E. Abrosimova, A.S. Aronin, A.V. Bezrukov, S.P. Pankratov and A.V. Serebryakov // *Physics of Metals* **4** (1982) 114.
- [40] A.S. Aronin, S.A. Ivanov and A.E. Yakshin // *Fizika Tverdogo Tela* **33** (1991) 2527.
- [41] G.E. Abrosimova and A.S. Aronin // *Physics of the Solid State* **51** (2009) 1665.
- [42] G. Abrosimova, A. Aronin and A. Budchenko // *Mater. Letters* **139** (2015) 194.
- [43] A.F. Skryshevskii, *Structure analysis of liquids and amorphous solids* (High School, Moscow, 1980).
- [44] A. Takeuchi and A. Inoue // *Materials Transactions* **46** (2005) 2817.
- [45] G.E. Abrosimova and A.S. Aronin // *Physics of Metals* **10** (1988) 47.
- [46] E. Pershina, G. Abrosimova, A. Aronin, D. Matveev and V. Tkatch // *Mater. Let.* **134** (2014) 60.
- [47] G.E. Abrosimova, A.S. Aronin, O.I. Barkalov and M.M. Dement'eva // *Physics of the Solid State* **55** (2013) 1773.